Three-dimensional structure of a mammalian thioredoxin reductase: Implications for mechanism and evolution of a selenocysteine-dependent enzyme

Tatyana Sandalova*, Liangwei Zhong†, Ylva Lindqvist*, Arne Holmgren†, and Gunter Schneider*‡

*Division of Molecular Structural Biology and †Medical Nobel Institute for Biochemistry, Department of Medical Biochemistry and Biophysics, Karolinska Institutet, S-171 77 Stockholm, Sweden

Edited by David R. Davies, National Institutes of Health, Bethesda, MD, and approved June 15, 2001 (received for review April 5, 2001)

Thioredoxin reductases (TrxRs) from mammalian cells contain an essential selenocysteine residue in the conserved C-terminal sequence Gly-Cys-SeCys-Gly forming a selenenylsulfide in the oxidized enzyme. Reduction by NADPH generates a selenolthiol, which is the active site in reduction of Trx. The three-dimensional structure of the SeCys498Cys mutant of rat TrxR in complex with $NADP^+$ has been determined to 3.0-Å resolution by x-ray crystallography. The overall structure is similar to that of glutathione reductase (GR), including conserved amino acid residues binding the cofactors FAD and NADPH. Surprisingly, all residues directly interacting with the substrate glutathione disulfide in GR are conserved despite the failure of glutathione disulfide to act as a substrate for TrxR. The 16-residue C-terminal tail, which is unique to mammalian TrxR, folds in such a way that it can approach the active site disulfide of the other subunit in the dimer. A model of the complex of TrxR with Trx suggests that electron transfer from NADPH to the disulfide of the substrate is possible without large conformational changes. The C-terminal extension typical of mammalian TrxRs has two functions: (*i*) it extends the electron transport chain from the catalytic disulfide to the enzyme surface, where it can react with Trx, and (*ii*) it prevents the enzyme from acting as a GR by blocking the redox-active disulfide. Our results suggest that mammalian TrxR evolved from the GR scaffold rather than from its prokaryotic counterpart. This evolutionary switch renders cell growth dependent on selenium.

Thioredoxin reductase (TrxR) (EC 1.6.4.5) is a member of the pyridine nucleotide–disulfide oxidoreductase family (1). Enzymes of this family, such as glutathione reductase (GR), lipoamide dehydrogenase, and trypanothione reductase, form homodimers, and each subunit contains a redox-active disulfide bond and a tightly bound FAD molecule. TrxR catalyzes reduction of Trx by NADPH. Trx is a ubiquitous 12-kDa protein, which in its dithiol form is the major disulfide reductase in cells (2, 3). Mammalian Trx is an essential protein (4) with a large number of functions in cell growth, such as thiol redox control of transcription factors, electron transport to ribonucleotide reductase, or defense against oxidative stress and apoptosis (2, 3). Trx and TrxR are present in all living cells from archea to human (3, 5). Whereas the essential features of Trx have been conserved during evolution, mammalian TrxRs are very different in structure and properties from the enzymes in bacteria, fungi, and plants (5, 6). For instance, mammalian TrxRs have a higher molecular mass (≥55 kDa) and a very broad substrate specificity (7) in contrast to the smaller (35 kDa) specific enzymes represented by the well characterized *Escherichia coli* TrxR (8). Mammalian TrxR directly reduces not only Trx from different species but also many nondisulfide substrates such as selenite (9), lipid hydroperoxides (10), and H_2O_2 (11) but not glutathione disulfide (GSSG) (5–7). Furthermore, the mammalian enzymes are inhibited by a number of clinically used drugs (review in ref. 12).

Cloning and sequencing of a putative human (13) and the bovine and rat cytosolic TrxR (14) revealed that they are similar to GR and not to the *Escherichia coli* TrxR enzyme. Compared with GR, the polypeptide chain of rat TrxR contains a C-terminal extension of 16 residues carrying a penultimate selenocysteine residue in the conserved sequence motif Gly-Cys-SeCys-Gly (14, 15). The selenocysteine residue is essential because its replacement with cysteine results in a mutant rat TrxR enzyme with about 1% activity with Trx as substrate and with a major loss in k_{cat} (11). Other activities of Se-containing TrxR and reduction of lipid hydroperoxides and H_2O_2 are lost in the Cys mutant, indicating an absolute requirement of selenium for these reactions. Because of the high nucleophilicity of selenolate, it is more susceptible to oxidation by H_2O_2 than thiols, a property that allows extension of the substrate spectrum toward hydroperoxides in the mammalian enzymes (11).

The truncated enzyme lacking the SeCys-Gly dipeptide is folded and contains FAD but is inactive, although titrations with NADPH yield the characteristic red-shifted thiolate-flavin charge transfer complex common for GR and mammalian TrxR (11, 16). Recently, the active site of mammalian TrxR was identified as a selenenylsulfide in the oxidized enzyme, and a selenolthiol is formed from the conserved Cys-SeCys sequence (17). The selenenyl sulfides in the oxidized human enzyme also have been confirmed (18).

TrxRs from mammalian sources belong to the rare group of enzymes containing selenocysteine, and few crystallographic studies of such enzymes have been performed, e.g., glutathione peroxidase (19) and formate dehydrogenase H (20). Here, we report the three-dimensional structure of the SeCys498Cys mutant of rat TrxR complexed with $NADP^+$. The crystal structure analysis reveals the overall fold of the enzyme, provides insights into the architecture of the active site, and allows a detailed comparison to other members of the pyridine nucleotide disulfide oxidoreductase family.

Materials and Methods

Protein Purification and Crystallization. Purification and crystallization of the SeCys498Cys mutant of rat TrxR in the presence of $NADP^+$ was carried out as described (21).

This paper was submitted directly (Track II) to the PNAS office.

Abbreviations: Trx, thioredoxin; TrxR, thioredoxin reductase; GR, glutathione reductase; GSSG, glutathione disulfide.

Data deposition: The crystallographic data for rat thioredoxin reductase have been deposited in the Protein Data Bank, www.rcsb.org (PDB ID code 1H6V).

‡To whom reprint requests should be addressed. E-mail: gunter@alfa.mbb.ki.se.

The publication costs of this article were defrayed in part by page charge payment. This article must therefore be hereby marked "*advertisement*" in accordance with 18 U.S.C. §1734 solely to indicate this fact.

Table 1. Data collection and refinement statistics

Resolution (Å)	30.0–3.0 (3.05–3.0)
Number of observations	212,337
Number of unique reflections	69,351
$\langle I/\sigma I \rangle$	11.0 (2.1)
Completeness	92.7 (77.6)
R_{sym}	9.5 (44.8)
Refinement statistics	
Number of atoms	23,104
R_{factor}	0.230
R_{free}	0.264
Overall *B* factor (Å^2)	22.5
Average *B* factor for C-terminal 16 residues (Å^2)	29.7
rms deviation bonds	0.013
rms deviation angles	1.970
Ramachandran plot, nonglycine residues in:	
Most favorable regions (%)	82.9
Additional allowed regions (%)	17.1
Disallowed regions (%)	0.0

Crystallographic Data Collection. X-ray data from a single crystal were collected to 3.0-Å resolution on a MAR345 image plate at a temperature of 100 K and a wavelength of 1.104 Å at the synchrotron beamline I711 (MAX Laboratory, Lund University, Sweden). Crystallization buffer containing 20% ethylene glycol was used as cryoprotectant. The x-ray data were processed and scaled with the HKL suite (22), and the statistics of the data set are given in Table 1. The crystals belong to the monoclinic space group $P2_1$ with cell dimensions $a = 78.9$ Å, $b = 140.5$ Å, $c = 170.8$ Å, and $\beta = 94.6°$.

Molecular Replacement and Crystallographic Refinement. A dimer of GR from human erythrocytes (PDB accession code 1GRA), with 36% sequence identity, was used as a search model for molecular replacement. Loop regions, where sequence alignments indicated differences in length/conformation, were removed from the model, and all residues that are not identical in rat TrxR and GR were replaced by alanine side chains. Molecular replacement was carried out by using the program EPMR (23). The calculations resulted in one single solution clearly above all others, giving three dimers in the asymmetric unit with a correlation coefficient of 0.41 and $r = 53.4\%$ and perfect crystal packing. The next best solution had a correlation coefficient of 0.354 and $r = 56\%$.

The coenzymes had been excluded from the search model, and the correctness of the molecular replacement solution was confirmed by electron density for FAD and the 2′phospho-AMP moiety of $NADP^+$ appearing at the expected positions. Refinement was performed with CNS (24). Five percent of the data were selected to monitor the progress of refinement by calculation of R_{free}. Manual rebuilding of the model was performed with the program O (25) based on σ_A-weighted $2F_o - F_c$ and $F_o - F_c$ electron density maps.

The electron density maps suggested that a tryptophan residue should replace Gly-53, which was confirmed by reexamination of the original sequencing data (14). Refinement continued with REFMAC5 (26), where the six subunits were considered as different TLS groups resulting in R_{free}/R values of 26.4/23.0%, respectively. Restrained noncrystallographic symmetry (CNS/REFMAC; 100 kcal·mol^{-1}·Å^{-2}/0.05 Å for main chain, and 50 kcal·mol^{-1}·Å^{-2}/0.5 Å for side-chain atoms) was used in the refinement.

Structural comparisons were carried out by using the program TOP with default parameters (27). Modeling of the binding of Trx to TrxR was performed manually with O (25). Figures were made with MOLSCRIPT (28), BOBSCRIPT (27), and RASTER3D (29, 30).

Results

Electron Density Map and Quality of the Model. The asymmetric unit of the crystal contains three dimers of rat TrxR. With a few exceptions, all polypeptide chains are well defined in electron density. The real space fit correlation to the electron density map is in the range 0.75 to 0.8 for all subunits except subunit C, where it is slightly less at 0.7. Less well defined regions of the polypeptide chain include several disordered residues at the N and C termini and two long surface loops (poor electron density for the side chains of residues 91–93 and 272–278, respectively). The final model includes residues 10–499 (subunits A and F), 9–495 (subunits B and D), 14–499 (subunit C), and 9–499 (subunit E), six FAD molecules, six $NADP^+$ molecules (2′-phospho-AMP moiety of $NADP^+$), and 15 water molecules. The electron

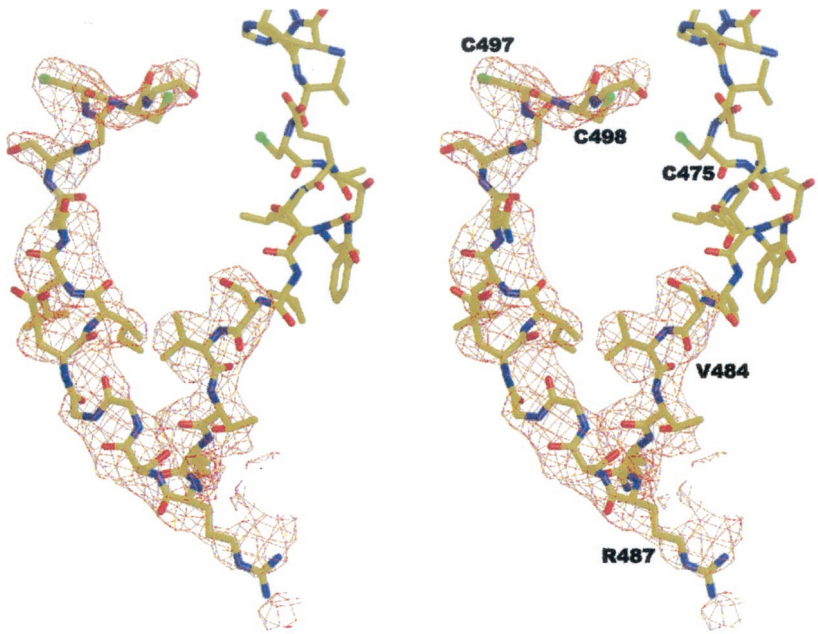

Fig. 1. Stereo view of an $F_o - F_c$ electron-density omit map for the C-terminal residues 484–499, contoured at 3.0 σ. The refined model is superimposed.

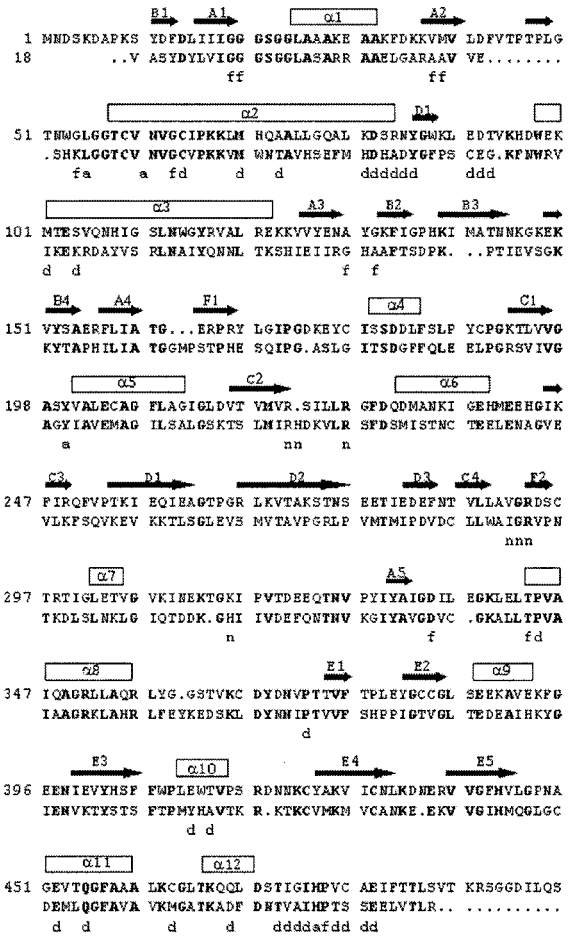

Fig. 2. Amino acid sequence and secondary structure elements. The secondary structure of rat TrxR is shown in the upper line. The nomenclature of the secondary structure elements is the same as used for GR (31); each α-helix is labeled by a sequential number, and each β-strand is indicated by a letter giving the sheet name and a number. Second line, amino acid sequence of rat TrxR; third line, sequence of human GR. Conserved residues are shown in bold letters. Possible functions of individual residues are indicated in the lower line. f, flavin binding; n, NADPH binding; d, participation in dimer interface; a, active site.

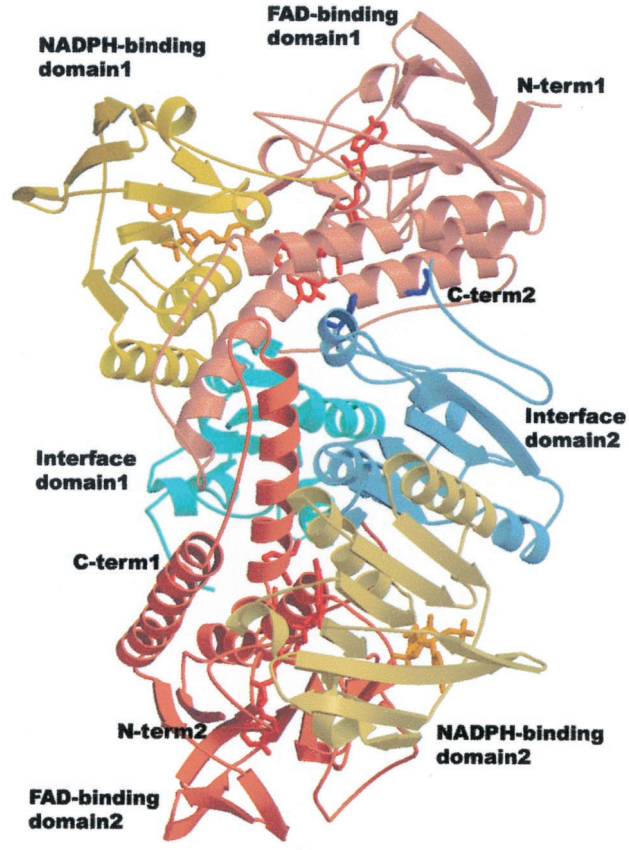

Fig. 3. Ribbon representation of the dimer of rat TrxR. The two subunits are shown in light or dark colors, respectively. Red, FAD binding domain; yellow, NADP binding domain; blue, interface domain. Bound FAD (red) and NADP (orange) are shown as ball-and-stick models.

density for FAD and the 2′-phospho-AMP moiety of $NADP^+$ is well defined in all subunits. There is, however, no electron density for the nicotinamide ring, and it was therefore not included in the model. Fig. 1 shows an omit map for the C-terminal tail of the polypeptide chain.

Overall Structure of Rat TrxR. The subunit of rat TrxR consists of the FAD binding domain (residues 1–163 and 297–367), the NADP(H) binding domain (residues 164–296), and the interface domain (residues 368–499) (Figs. 2 and 3). The FAD and NADP binding domains have similar folds; each domain contains a central five-stranded parallel β-sheet and a three-stranded β-meander that is packed against the larger β-sheet. The other side of the parallel sheet is covered by several α-helices. These domains, variants of the Rossmann fold, bind NADP(H) and FAD in a manner characteristic of this fold (31). In rat TrxR, there is an insertion in the FAD binding domain between strand A2 and helix α2, which forms two small β-strands. The active disulfide, formed by Cys-59 and Cys-64 located on helix α2, shows the same distortion at this position as other pyridine nucleotide disulfide oxidoreductases. The redox-active disulfide of rat TrxR is thus located in the FAD domain, as in GR (31), and not in the NADP binding domain as in prokaryotic TrxR (32), in agreement with conclusions based on amino acid sequence comparisons (14).

The third domain, the interface domain, contains an antiparallel five-stranded β-sheet E flanked on both sides by four helices. This domain participates in subunit–subunit interactions and forms a large part of the dimer interface.

The C-terminal extension with the characteristic motif Gly-Cys-SeCys-Gly carrying the essential selenocysteine residue (Fig. 4) is unique for mammalian TrxRs. Residues 470–483, which correspond to the last residues of GR, have the same conformation as in GR. The first three residues of the extension, Val-484–Thr-485–Lys-486, continue in the direction toward the surface of the molecule, running antiparallel to the edge strand of β-sheet E of the interface domain. At the position of Arg-487, the chain makes a sharp turn and runs parallel to the outer strand in sheet F. Another turn at position Ser-495 directs the remaining part of the chain toward the active site of the second subunit. The last residues form mainly van der Waals interactions with enzymic groups at the active site. Noteworthy is the interaction of main-chain oxygen atom of Cys-498 with the side chain of Tyr-116. The latter residue is conserved in GR and interacts with bound glutathione. The C-terminal carboxyl group of the chain is anchored to the protein via a salt bridge with the side chain of Lys-29.

The active sites of TrxR are located at the interface between the two subunits, and the dimer is therefore the functional unit of the enzyme. Out of the 30 residues forming the interface region of rat TrxR, 10 are conserved in GR (Fig. 2).

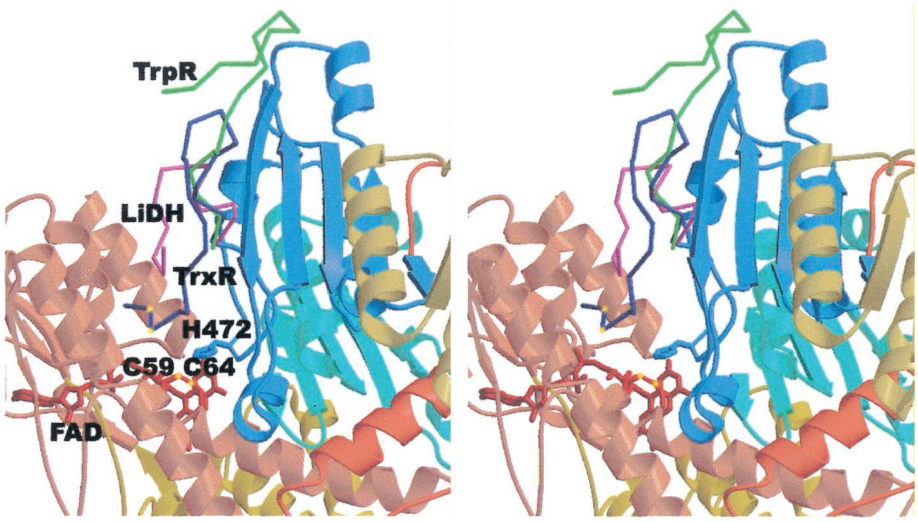

Fig. 4. Stereo view of the C-terminal extensions in enzymes of the pyridine nucleotide–disulfide oxidoreductase family. The structure of rat TrxR is shown as a ribbon model (color coding as in Fig. 3). The C-terminal extensions are shown as Cα traces (LiDH, dihydrolipoamide dehydrogenase, magenta; TrpR, trypanothione reductase, green; TrxR, rat TrxR, blue). The positions of the catalytic disulfide (Cys-59–Cys-64), and the cysteine residues Cys-497 and Cys-498 in the C-terminal tail of TrxR are indicated by yellow spheres.

Comparison with Related Enzymes. Enzymes most similar in amino acid sequence, fold, and topology to rat TrxR are GR (31, 33), trypanothione reductase (34), and dihydrolipoamide dehydrogenase (35). Dihydrolipoamide dehydrogenase and trypanothione reductase also have C-terminal extensions of the polypeptide chain (Fig. 4). In trypanothione reductase, the conformation of the C-terminal residues is completely different from rat TrxR, forming two additional antiparallel β-strands in the central β-sheet of the interface domain, which are thus far from the active site. In lipoamide dehydrogenase, the last residues form an arm that protrudes into the subunit interface (35) toward the active site similar to rat TrxR, but the conformation of the C termini is quite different in these two enzymes (Fig. 4).

All insertions and deletions in the polypeptide chains of the compared enzymes of the family occur in loops at the surface of the protein. Two insertions in TrxR, comprising residues 44–54 and 142–149, form two β-hairpins and shield the adenine part of the FAD molecule, which is more buried in TrxR than in GR. Insertions in the NADP binding domain occur at the N and the C termini of the β-strand E2, thus extending this strand.

FAD and NADP Binding. The cofactor FAD is tightly, but noncovalently, bound to rat TrxR, and almost all FAD atoms that can act as hydrogen bond donors or acceptors are engaged in hydrogen bonds. As in all other pyrimidine nucleotide disulfide oxidoreductases of known structure, the FAD molecule has an extended conformation. Most of the interactions between FAD and the enzyme are made by residues from the FAD binding domain and are very conserved in the family (Fig. 2).

The coenzyme NADP is bound in a cleft between the FAD and NADP binding domains with the adenine moiety packed against the central β-sheet of the NADP binding domain. The rest of the molecule extends toward the isoalloxazine ring of FAD. Besides Tyr-200, there are only two other conserved residues in the NADP binding site: Arg-221 and Arg-226. Both residues form hydrogen bonds with the 2′ phosphate of NADP and are thus involved in recognition of NADP versus NAD.

The GSSG Binding Site Is Conserved in Mammalian TrxR. In GR, residues from four helices of one subunit and the C-terminal part of the other subunit form the substrate binding site. Because GR and rat TrxR differ in substrate specificity, it was expected that their substrate binding sites should be different. However, residues that form hydrogen bonds with glutathione in GR are conserved in rat TrxR. In human GR, direct hydrogen bonds were found between GSSG and the side chains of residues Ser-30, Arg-37, Tyr-114, Arg-347, His-467, and Glu-473 (36). Arg-37 and Arg-347 anchor the carboxyl group of GSSG, and the hydroxyl groups of Tyr-116 and Ser-30 form hydrogen bonds with main-chain atoms of GSSG. With the exception of the conservative substitution R37K (we also note that this side chain is not conserved in GR), all of these residues are present in rat TrxR. Whereas Arg-37 in GR is anchoring the carboxyl group of glutathione inside the active site, the corresponding residue, Lys-29, in TrxR forms a salt bridge with the terminal carboxyl group. The last residues of the C-terminal part of the polypeptide chain are partly occupying a possible glutathione binding site and thus prevent access of GSSG to the catalytic disulfide at the active site (Fig. 5).

Redox-Active Disulfide. The electron density map clearly shows the presence of a disulfide bond between Cys-59 and Cys-64. The isoalloxazine ring of FAD packs against this disulfide, and the sulfur atom of Cys-64 is close to the isoalloxazine ring (3.6 Å), suggesting that this residue is responsible for the formation of the thiolate–flavin charge transfer complex.

Interaction with Trx. There are no experimental data to suggest which residues participate in the binding of Trx to mammalian TrxR. We modeled the structure of this complex by docking Trx at the enzyme surface, minimizing the distance between its disulfide and the C terminal of rat TrxR (Fig. 6). This docking was possible without introducing steric clashes, and no conformational changes involving main chain atoms of Trx or TrxR were necessary. Based on this crude model, a putative binding site for Trx can be proposed, which involves residues from both subunits of TrxR. The binding area is formed by residues from helix 4 of one subunit and residues from the C-terminal tail and the loop connecting helix 10 and strand E4 of the second subunit. In the model, hydrophobic residues of Trx dock to a nonpolar surface of mammalian TrxR. Residue Trp-31 is packed between Gly-115, Val-118, and Cys-497; Pro-34 of Trx stacks onto the side chain of Trp-407. The interface contains a number of charged residues, which may form salt bridges. Residues Arg-117, Arg-121, and Lys-124 of TrxR could interact with the negatively charged residues Asp-60, Asp-61, and Asp-64 at the surface of Trx. Lys-72 of Trx and Glu-491 of TrxR could form an additional ionic interaction.

Discussion

The present study has revealed a striking similarity in three-dimensional structure between rat TrxR and GR. It also verifies

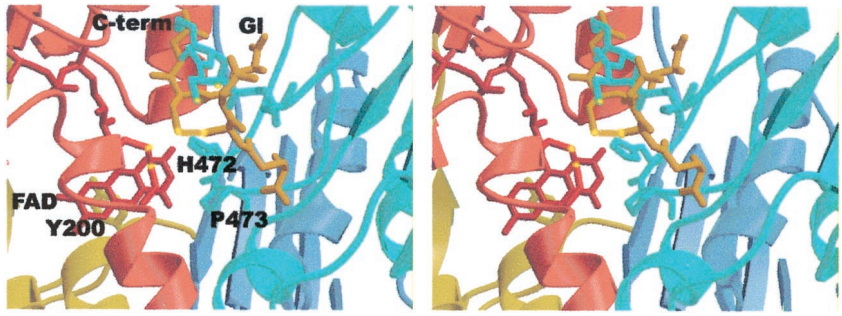

Fig. 5. Active site of the SeCys498Cys mutant of rat TrxR (color coding as in Fig. 3). The observed conformation of Tyr-200 shields FAD from the solvent and hinders proper binding of the nicotinamide ring of $NADP^+$. The position of oxidized glutathione (Gl, brown) was derived from a superposition of the structures of rat TrxR and the complex of GR with glutathione (36). The positions of the sulfur atoms of glutathione, the catalytic disulfide (Cys-59–Cys-64), and the cysteine residues Cys-497 and Cys-498 are indicated by yellow spheres.

a previous proposal of the packing of the two subunits in a head-to-tail arrangement (17). Particularly noteworthy is the conservation in TrxR of active site residues that participate in binding of the substrate glutathione in GR, despite the differences in substrate specificity. The conservation of three-dimensional structure in the two enzymes strongly supports suggestions that mammalian TrxR may have evolved from the evolutionary more recent GR rather than from prokaryotic TrxRs (17, 37). Evolution of a novel TrxR from a GR scaffold involved extension of the electron transfer chain to the surface of the enzyme by the incorporation of another redox center at the C-terminal part of the chain. In some species, for instance *Plasmodium falciparum*, this center consists of a Cys-XXXX-Cys motif (37), whereas in mammals it is a Cys-SeCys peptide. In both cases, this part of the chain can act as a swinging arm that transports redox equivalents from the buried catalytic disulfide of TrxR to the protein substrate, Trx. Prevention of glutathione binding to TrxR is not achieved primarily by mutations of substrate binding residues, as one might have anticipated, but through steric hindrance via the C-terminal tail, which blocks access to the catalytic disulfide of TrxR. One could therefore expect that a truncated version of mammalian TrxR might be active as a GR.

The evolutionary distance between TrxR from prokaryotes and lower eukaryotes on one hand and the enzyme from higher eukaryotes on the other hand is further emphasized by the fact that catalysis occurs in a completely different manner. TrxR from *E. coli* shows a large rearrangement of the FAD and NADPH binding domains as part of the catalytic cycle (38). In mammalian TrxR, however, the orientation of these domains as seen in the crystals would allow electron transfer from NADPH to the disulfide of Trx without the necessity to invoke similar large conformational changes.

The first steps of catalysis, reduction by NADPH and formation of a charge-transfer intermediate (Fig. 7), are common to GR and mammalian TrxR and do not depend on the presence of the SeCys-Gly peptide of mammalian TrxR (11). The second part of the reaction, however, is different. In oxidized wild-type enzyme, a selenenylsulfide bond was found between Cys-497 and SeCys-498, which can be reduced upon addition of NADPH (14, 16, 17). It has therefore been proposed that in mammalian TrxR,

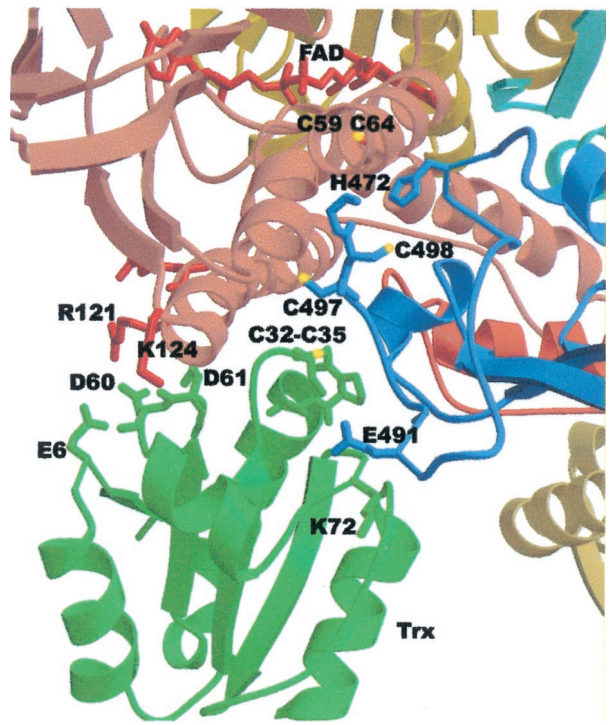

Fig. 6. Model of the complex of rat TrxR with human Trx. Color coding for TrxR is as in Fig. 3, Trx is shown in green. Residues at the Trx–TrxR interface are shown as stick models. The positions of the sulfur atoms of the catalytic disulfide (Cys-59–Cys-64) and the cysteine residues Cys-32, Cys-35, Cys-497, and Cys-498 are indicated by yellow spheres.

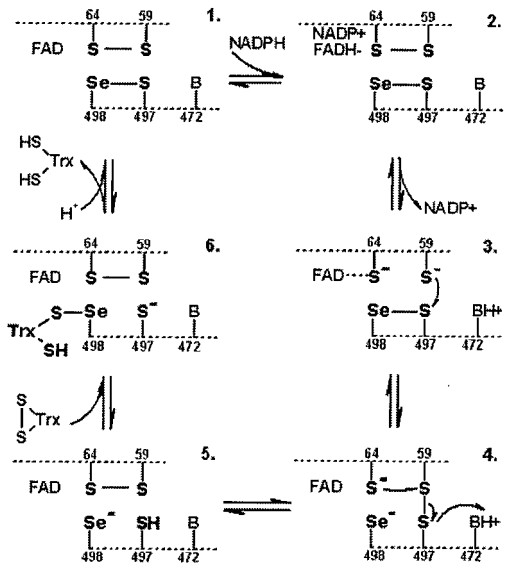

Fig. 7. Postulated reaction mechanism for mammalian TrxR.

BIOCHEMISTRY

the conserved Cys-497–SeCys-498 motif acts as a second redox center and that electrons are transferred from the redox-active disulfide via the redox center at the C terminal to the substrate, Trx (14, 17, 37). This proposal is consistent with the observed three-dimensional structure of mammalian TrxR, which represents compound 5 in Fig. 7. The conformation of the very C terminal can be modeled in such a way that it approaches the redox-active disulfide Cys-59–Cys-64 close enough for electron transfer without steric clashes, decreasing the distance between Cys-59 and Cys-497 from 12 Å to 3 Å. This conformational change involves mainly residues Ser-495–Cys-498, where the largest movement is that of Cys-497 (about a 5-Å displacement of the Cα atom). The charge interaction between the C-terminal carboxyl group of Gly-499 and the side chain of Lys-29 can be maintained in the two conformations.

In such a model of the oxidized form of the Cys-497–SeCys-498 motif, the selenium atom would be located very close to the side chain of the conserved His-472, and the imidazole group could participate in proton transfer to Cys-497. After reduction, the C-terminal tail could then move away from the catalytic site to a position at the surface of the enzyme, as seen in the structure presented here, and interact with the bound substrate, Trx. The model of the TrxR–Trx complex is consistent with a mechanistic scenario for the dithiol–disulfide exchange reaction put forward previously (17). In this step of the reaction, the selenolate anion attacks the disulfide of Trx. The resulting enzyme, Trx-mixed selenenylsulfide (Fig. 7, compound 6), is then attacked by Cys-497 to regenerate the selenenylsulfide.

This proposal of a C terminus switching between a less accessible, oxidized, and surface-exposed reduced Cys-SeCys motif as part of the catalytic cycle of rat TrxR is consistent with proteolysis data. The reduced enzyme is susceptible to degradation by carboxypeptidase Y (14) or trypsin (39). Loss of activity is caused by removal of the SeCys residue, indicating a surface-exposed conformation of the C terminal. In the oxidized enzyme, the last residues are buried at the active site and are not accessible to the protease or to chemical modification (14, 18).

We acknowledge access to synchrotron radiation at beamline 711, MAX Laboratory, University of Lund, Sweden; we thank Yngve Cerenius for assistance at the beamline. This work was supported by grants from the Medical Research Council, Karolinska Institutet, and the Natural Science Research Council.

1. Williams, C. H., Jr. (1992) in *Chemistry and Biochemistry of Flavoenzymes*, ed. Müller, F. (CRC, Boca Raton, FL), Vol. III, pp. 121–211.
2. Holmgren, A. (1985) *Annu. Rev. Biochem.* **54,** 237–271.
3. Arnér, E. S. J. & Holmgren, A. (2000) *Eur. J. Biochem.* **267,** 6102–6109.
4. Matsui, M., Oshima, M., Oshima, H., Takaku, K., Maruyama, T., Yodoi, J. & Taketo, M. M. (1996) *Dev. Biol.* **178,** 179–185.
5. Luthman, M. & Holmgren, A. (1982) *Biochemistry* **21,** 6628–6633.
6. Holmgren, A. (1989) *J. Biol. Chem.* **264,** 13963–13966.
7. Arnér, E. S. J., Zhong, L. & Holmgren, A. (1999) *Methods Enzymol.* **300,** 226–239.
8. Waksman, G., Krishna, T. S. R., Sweet, R. M., Williams, C. H., Jr. & Kuriyan, J. (1994) *J. Mol. Biol.* **236,** 800–816.
9. Kumar, S., Björnstedt, M. & Holmgren, A. (1992) *Eur. J. Biochem.* **207,** 435–439.
10. Björnstedt, M., Hamberg, M., Kumar, S., Xue, J. & Holmgren, A. (1995) *J. Biol. Chem.* **270,** 11761–11764.
11. Zhong, L. & Holmgren, A. (2000) *J. Biol. Chem.* **275,** 18121–18128.
12. Becker, K., Gromer, S., Schirmer, R. H. & Müller, S. (2000) *Eur. J. Biochem.* **267,** 6118–6125.
13. Gasdaska, P. Y., Gasdaska, J. R., Cochran, S. & Powis, G. (1995) *FEBS Lett* **373,** 5–9.
14. Zhong, L., Arnér, E. S. J., Ljung, J., Åslund, F. & Holmgren, A. (1998) *J. Biol. Chem.* **273,** 8581–8591.
15. Gladyshev, V. N., Jeang, K. T. & Stadtman, T. C. (1996) *Proc. Natl. Acad. Sci. USA* **93,** 6146–6151.
16. Arscott, L. D., Gromer, S., Schirmer, R. H., Becker, K. & Williams, C. H., Jr. (1997) *Proc. Natl. Acad. Sci. USA* **94,** 3621–3626.
17. Zhong, L., Arnér, E. S. J. & Holmgren, A. (2000) *Proc. Natl. Acad. Sci. USA* **97,** 5854–5859. (First Published May 9, 2000; 10.1073/pnas.100114897)
18. Lee, S. R., Bar-Noy, S., Kwon, J., Levine, R. L., Stadtman, T. C. & Rhee, S. G. (2000) *Proc. Natl. Acad. Sci. USA* **97,** 2521–2526. (First Published February 25, 2000; 10.1073/pnas.050579797)
19. Ren, B., Huang, W., Åkesson, B. & Ladenstein, R. (1997) *J. Mol. Biol.* **268,** 869–885.
20. Boyington, J. C., Gladyshev, V. N., Khangulov, S. V., Stadtman, T. C. & Sun, P. D. (1997) *Science* **275,** 1305–1308.
21. Zhong, L., Persson, K., Sandalova, T., Schneider, G. & Holmgren, A. (2000) *Acta Crystallogr. D* **56,** 1191–1193.
22. Otwinowski, Z. (1993) in *Proceedings of the CCP4 Study Weekend: Data Collection and Processing*, eds. Sawyer, L., Isaacs, N. & Baily, S. (Science and Engineering Research Council Daresbury Laboratory, Warrington, U.K.), pp. 56–62.
23. Kissinger, C. R., Gehlhaar, D. K. & Fogel, D. B. (1999) *Acta Crystallogr. D* **55,** 484–491.
24. Brünger, A. T., Adams, P. D., Clore, G. M., DeLano, W. L., Gros, P., Grosse-Kunstleve, R. W., Jiang, J.-S., Kuszewski, J., Nilges, M., Pannu, N. S., *et al*. (1998) *Acta Crystallogr. D* **54,** 905–921.
25. Jones, T. A., Zou, J., Cowan, S. & Kjeldgaard, M. (1991) *Acta Crystallogr. A* **47,** 110–119.
26. Winn, M. D., Isupov, M. N. & Murshudov, G. N. (2001) *Acta Crystallogr. D* **57,** 122–133.
27. Lu, G. (2000) *J. Appl. Crystallogr.* **33,** 176–183.
28. Kraulis, P. (1991) *J. Appl. Crystallogr.* **24,** 946–950.
29. Esnouf, R. M. (1997) *J. Mol. Graphics Mod.* **15,** 133–138.
30. Merrit, E. A. & Murphy, M. E. P. (1994) *Acta Crystallogr. D* **50,** 869–873.
31. Schulz, G. E., Schirmer, R. H., Sachsenheimer, W. & Pai, E. F. (1978) *Nature (London)* **273,** 120–124.
32. Kuriyan, J., Krishna, T. S., Wong, L., Guenther, B., Pahler, A., Williams, C.H., Jr. & Model, P. (1991) *Nature (London)* **352,** 172–174.
33. Mittl, P. R. & Schulz, G. E. (1994) *Protein Sci.* **3,** 799–809.
34. Bond, C. S., Zhang, Y., Berriman, M., Cunningham, M. L., Fairlamb, A. H. & Hunter, W. N. (1999) *Structure (London)* **7,** 81–89.
35. Mattevi, A., Obmolova, G., Sokatch, J. R., Betzel, C. & Hol, W. G. (1992) *Proteins* **13,** 336–351.
36. Karplus, P. A. & Schulz, G. E. (1989) *J. Mol. Biol.* **210,** 163–180.
37. Williams, C. H., Jr., Arscott, L. D., Müller, S., Lennon, B. W., Ludwig, M. L., Wang, P.-F., Veine, D. M., Becker, K. & Schirmer, R. H. (2000) *Eur. J. Biochem.* **267,** 6110–6117.
38. Lennon, B. W., Williams, C.R., Jr. & Ludwig, M. L. (2000) *Science* **289,** 1190–1194.
39. Gromer, S., Wissing, J., Behne, D., Ashman, K., Schirmer, R. H., Flohé, L. & Becker, K. (1998) *Biochem. J.* **332,** 591–592.